High-Resolution Single-Shot Spiral Imaging using Magnetic Field Monitoring and its Application to Diffusion Weighted MRI

Bertram J. Wilm[1,2], Christoph Barmet[1,2], Simon Gross[1], Lars Kasper[1], Johanna Vannesjo[1], Maximilian Haeberlin[1], Benjamin Dietrich[1], David Brunner[1], Thomas Schmid[1], and Klaas P. Pruessmann[1]

[1]*Institute for Biomedical Engineering, University & ETH, Zurich, Zurich, Switzerland,* [2]*Skope Magnetic Resonance Technologies, Zurich, Zurich, Switzerland*

Introduction: Spiral acquisition holds great potential in single-shot MRI [1-5], since it allows for shortest possible echo times and is among the fastest ways to encode a given resolution and FOV. Thereby spiral imaging enables to improve the achievable signal-to-noise ratio, temporal resolution, robustness against motion, and the increased bandwidth-per-pixel prompts expectations to diminish sensitivity against chemical shift and static B_0 off-resonance artifacts. Despite these theoretical benefits, single-shot spiral readouts are refrained from being used in practice due to their sensitivity to any encoding deficiencies such as gradient delays, concomitant fields and (higher-order) eddy currents, static B_0 off-resonance and field drifts during the scan.

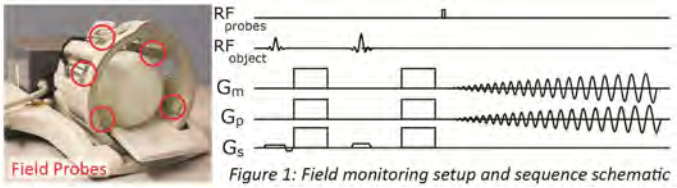

Figure 1: Field monitoring setup and sequence schematic

To overcome these limitations we propose the application of higher-order magnetic field monitoring [6], where all dynamic encoding fields are recorded during data acquisition and are subsequently incorporated into higher-order image reconstruction [7]. To demonstrate the benefit of this method, we present its application to high-resolution diffusion imaging where the eddy current situation is particularly challenging.

Methods: Imaging was performed on a 3T Achieva System (Philips Healthcase, Best, The Netherlands) using an 8-element head coil array and 16 NMR field probes mounted to the head coil (Fig.1, left). Single-shot spiral scans (FOV: $(230\text{mm})^2$, resolution: $(1.3\text{mm})^2$, slice thickness: 2 mm, TE: 34ms, diffusion weighting (DW) ($b=1000$ s/mm^2, 12 orientations + b_0) were acquired in vitro (spherical phantom, 20 cm diameter, low-diffusive silicon oil) and in a healthy subject in a transverse plane. To achieve robustness against static B_0 off-resonance, the k-space undersampling factor was set to 4, which resulted in a total readout duration of 32 ms. In addition two gradient echo sequences (resolution: $(2\text{ mm})^2$, slice thickness: 4 mm, TE: 2.4 ms and 2.9 ms) were acquired in the same slices to serve as an input for receive coil sensitivity and static ΔB_0-maps. In all scans the encoding fields were recorded simultaneously with the image data acquisition using 16 NMR field probes [6]. The field probes were excited after the diffusion weighting gradients in the spiral scans (Fig. 1, right) and after slice selection in the FFE scans. From the probes data, a 3rd-order k-space trajectory was calculated [6] by expansion on concomitant field [8] and spherical harmonics basis functions [7]. The FFE images and resulting SENSE and ΔB_0 maps were reconstructed [7] prior to the DW images on the monitored trajectory. To demonstrate the effect of higher-order image reconstruction, the in-vitro DW data was reconstructed on the nominal trajectory, using monitored 0th-1st order encoding and with full 3rd-order encoding with SENSE and ΔB_0 correction [7]. Finally, quantitative maps were calculated from 3rd-order reconstructed in-vivo DTI dataset without prior image co-registration.

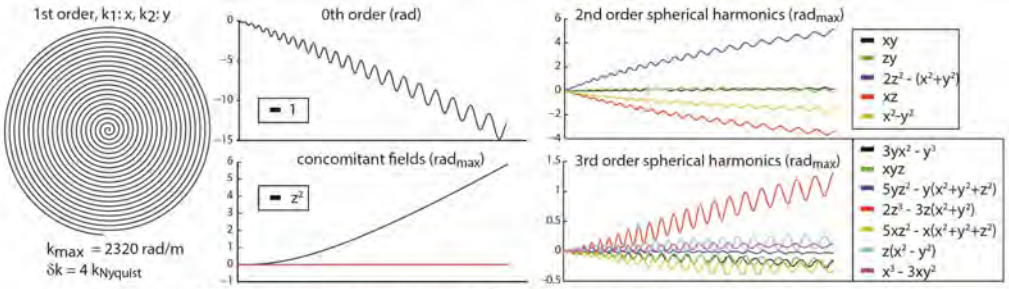

Figure 2: Measured field evolution during data acquisition of a DW single-shot spiral (duration: 32 ms). Higher-order terms are scaled to show the maximum effect in radian (rad_{max}) within the imaging volume relating to each basis function.

Results: Figure 1 shows the recorded field evolution during a diffusion weighted spiral acquisition. In addition to the first order (gradient) encoding, global B_0 changes (0th order) as well as oscillatory terms probably relating to gradient coil coupling are visible (0th-3rd order). The dominating higher-order effects originate from concomitant fields and long-lived DW eddy current fields that significantly contribute to image encoding with a maximum effect of ~6 rad within the imaging volume.

Image reconstruction on the nominal trajectory resulted in strong blurring artifacts and incongruence of the DW images (Fig.3 top). The incorporation of monitored 0th and 1st order fields drastically improved image quality of the images (Fig.3 middle). The DW images showed remaining artifacts, leading to incongruence among the images (Fig.3 middle, b_0-DW). Incorporating higher-order fields removed the remaining image artifacts and resulted in a congruent data set (Fig.3 bottom). The high-resolution in vivo data (Fig. 4) did not show perceivable blurring or aliasing artifacts nor artifacts relating to geometrical incongruence of the individual DW images.

Discussion and Conclusion:

As compared to previous findings, the image quality of the single-shot spiral images was significantly improved. This can be attributed to the accurate encoding model for the DTI data as well as well as consistent encoding between all data sets and the SENSE and ΔB_0 maps. In addition, robustness against ΔB_0-blurring artifacts was supported by using a high SENSE-factor of 4. The in-vitro results show that the incorporation of higher-order fields is necessary to fully correct for DW induced distortions. The echo time of only 34 ms for a b-factor of 1000 s/mm^2, leads to a nominal increase of SNR of 30-80% as compared to single-shot EPI for typical image resolutions in DTI. The high SNR efficiency and the motion robustness make this sequence ideal for its use in clinical DWI and research.

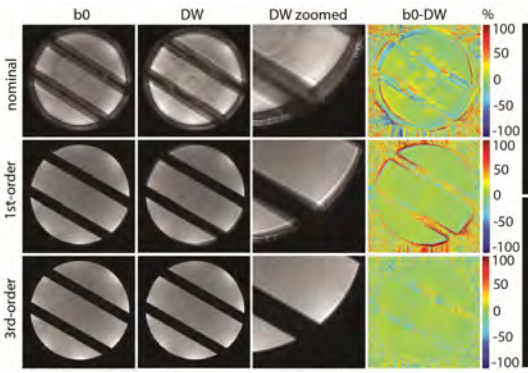

Figure 3 : Single-shot spiral images. Effect of encoding input to image reconstruction.

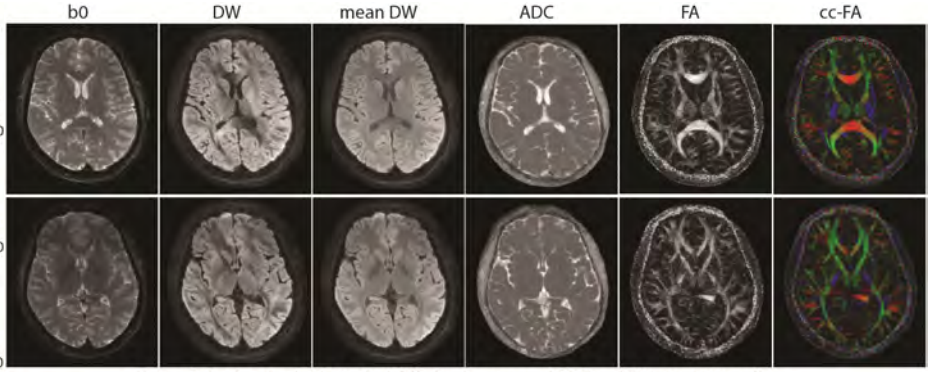

Figure 4 : In-vivo single-shot spiral diffusion images and ADC and FA maps in two slices

References: [1]: Block et al. JMRI (21) 2005, **[2]:** Glover et al. Neuroimage (63) 2012, **[3]:** Weiger et al. MRM (48) 2002, **[4]:** Heberlein et al. MRM (55) 2006, **[5]:** Heidemann et al. MRM (56) 2006, **[6]:** Barmet et al. MRM (63) 2012, **[7]:** Wilm et al. MRM (63) 2012, **[8]:** Bernstein et al., MRM (39(2)) 1998